ACCOUNTS
of chemical research

Protein Dynamics Studied with Ultrafast Two-Dimensional Infrared Vibrational Echo Spectroscopy

MEGAN C. THIELGES† AND MICHAEL D. FAYER*
Department of Chemistry Stanford University, Stanford, California 94305, United States

RECEIVED ON OCTOBER 29, 2011

CONSPECTUS

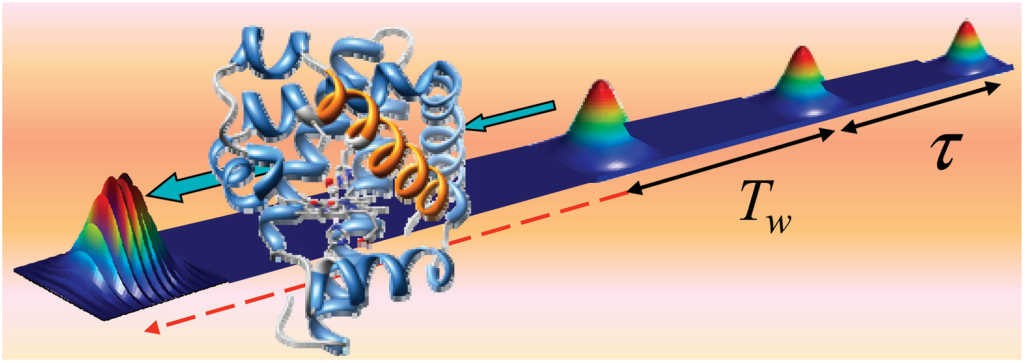

Proteins, enzymes, and other biological molecules undergo structural dynamics as an intrinsic part of their biological functions. While many biological processes occur on the millisecond, second, and even longer time scales, the fundamental structural dynamics that eventually give rise to such processes occur on much faster time scales. Many decades ago, chemical kineticists focused on the inverse of the reaction rate constant as the important time scale for a chemical reaction. However, through transition state theory and a vast amount of experimental evidence, we now know that the key events in a chemical reaction can involve structural fluctuations that take a system of reactants to its transition state, the crossing of a barrier, and the eventual relaxation to product states. Such dynamics occur on very fast time scales.

Today researchers would like to investigate the fast structural fluctuations of biological molecules to gain an understanding of how biological processes proceed from simple structural changes in biomolecules to the final, complex biological function. The study of the fast structural dynamics of biological molecules requires experiments that operate on the appropriate time scales, and in this Account, we discuss the application of ultrafast two-dimensional infrared (2D IR) vibrational echo spectroscopy to the study of protein dynamics. The 2D IR vibrational echo experiment is akin to 2D NMR, but it operates on time scales many orders of magnitude faster. In the experiments, a particular vibrational oscillator serves as a vibrational dynamics probe. As the structure of the protein evolves in time, the structural changes are manifested as time-dependent changes in the frequency of the vibrational dynamics probe. The 2D IR vibrational echo experiments can track the vibrational frequency evolution, which we then relate to the time evolution of the protein structure. In particular, we measured protein substate interconversion for mutants of myoglobin using 2D IR chemical exchange spectroscopy and observed well-defined substate interconversion on a sub-100 ps time scale. In another study, we investigated the influence of binding five different substrates to the enzyme cytochrome $P450_{cam}$. The various substrates affect the enzyme dynamics differently, and the observed dynamics are correlated with the enzyme's selectivity of hydroxylation of the substrates and with the substrate binding affinity.

I. Introduction

In recent years, the study of the dynamics of biological molecules undergoing structural changes on a wide range of time scales, from femtoseconds to milliseconds, has been the topic of considerable interest.[1−4] Biological function requires protein structural changes on a variety of time scales.[1,2] Accumulating evidence suggests that very fast structural fluctuations on subnanosecond time scales can

Published on the Web 03/20/2012 www.pubs.acs.org/accounts
10.1021/ar200275k

be intimately related to protein function manifested on much longer time scales.[5−9] For example, subnanosecond time scale motions have been implicated in the thermodynamics and specificity of protein−protein binding[9,10] and allostery.[8] The two-dimensional infrared (2D IR) spectroscopic experiments discussed herein suggest that motions on the picosecond time scale contribute to the selectivity of hydroxylation by cytochrome $P450_{cam}$.[7] Understanding the structural dynamics of biomolecules can provide valuable information regarding the relationship between structure and function.[5,11,12]

The energy landscapes of proteins are complex and frequently contain a number of local minima of similar energy. Each local minimum reflects a particular conformational state where the protein adopts a distinct structure.[5] Under thermal equilibrium conditions, protein structures fluctuate and continually switch among their conformational states. In addition to interconversion between distinct energy minima, proteins undergo structural fluctuations within a particular conformational state.

Two-dimensional infrared (2D IR) vibrational echo spectroscopy can measure protein structural fluctuations on fast times scales.[7,13−16] Applications of 2D IR spectroscopy to biomolecules include studies of protein structure, dynamics, and folding.[7,15−21] Here we discuss two related 2D IR techniques that have been employed for the study of protein dynamics. The first is chemical exchange spectroscopy, which provides a direct observable for monitoring the interconversion between two distinct protein conformations. The second is the measurement of spectral diffusion, which is the time evolution of the frequency of the vibrational probe within the inhomogeneous distribution of states reflected in the vibrational absorption line width. The time-dependent frequency changes are caused by structural fluctuations of the vibrational probe and its environment. The experimental measurement of spectral diffusion is used to determine the frequency−frequency correlation function (FFCF), which is the connection between the experimental observables and the underlying dynamics of the system.[22]

II. Experimental Procedures

Herein are discussed example studies of two heme proteins: mutants of myoglobin (Mb) and cytochrome $P450_{cam}$ ($P450_{cam}$). CO binds the active sites of both heme proteins and displays a strong vibrational stretching transition at ∼1950 cm^{-1}. The CO serves as the vibrational probe of the surrounding protein dynamics.

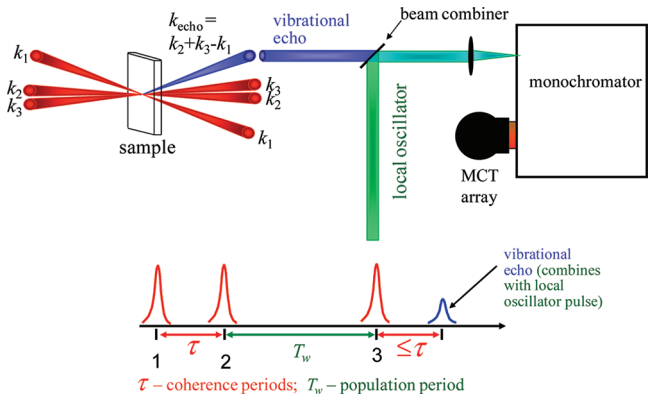

FIGURE 1. Two-dimensional IR experimental pulse sequence, geometry, and detection.

The laser system used for these experiments consists of a Ti:sapphire oscillator and regenerative amplifier pumping an optical parametric amplifier and difference frequency stage to produce ∼90 fs pulses at ∼5 μm (1950 cm^{-1}). The frequency of the IR is tuned to the transition frequency of the CO stretch for the protein under study. Because the pulses are short, the bandwidth spans the ground state to first vibrational excited state (0−1) transition as well as the first to second excited state transition (1−2).

In 2D IR vibrational echo experiments,[22] the IR beam is split into three excitation pulses and a fourth beam, the local oscillator (LO) (Figure 1). The three excitation pulses are time ordered, with pulses 1 and 2 traveling along variable delay stages. The first pulse creates a coherence consisting of a superposition of the $v=0$ and $v=1$ vibrational levels. During the evolution period τ, the phase relationships between the oscillators decay. The second pulse reaches the sample at time τ and creates a population state in either $v=0$ or $v=1$. A time T_w (the waiting period) elapses before the third pulse arrives at the sample to create another coherence that partially restores the phase relationships. Rephasing of the oscillators causes emission of a vibrational echo signal. For very short T_w times, the echo will be emitted at a time $t \approx \tau$ after the third pulse, and for increasingly longer T_w times, it will appear increasingly nearer the time of the third pulse. During T_w, the frequencies of the CO molecules change (chemical exchange[14,21,23] or spectral diffusion[7,15,16]) as they sample different environments due to the structural evolution of the proteins.[24−26] The echo signal is spatially and temporally overlapped with the LO for heterodyned detection, which provides both signal amplification and phase information. The heterodyned signal is frequency dispersed by a monochromator and detected with an array detector. Taking the spectrum of the signal provides the

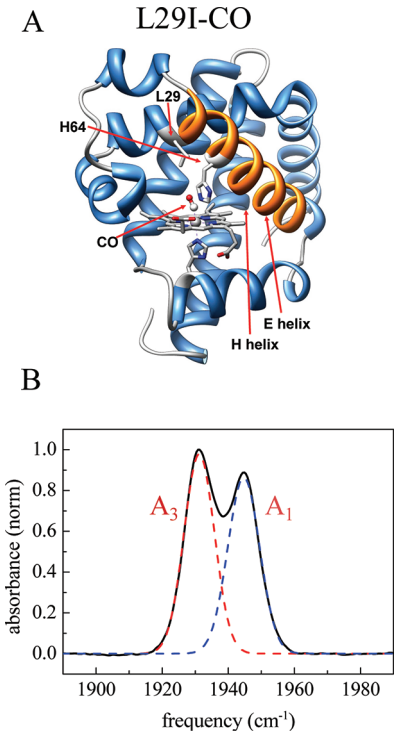

FIGURE 2. (A) Structure of Mb L29I (pdb id 1MWC) and (B) FT IR spectrum of CO in L29I Mb.

vertical axis (ω_m axis) in the 2D spectrum. At each ω_m frequency, scanning τ produces a temporal interferogram. Numerical Fourier transforms of these interferograms give the horizontal axis (ω_τ axis). Then T_w is changed and another 2D spectrum is recorded. The time evolution of the 2D spectra provides the information on the system dynamics.

III. Results and Discussion

A. Substate Switching in Myoglobin–CO Observed with Chemical Exchange Spectroscopy. The ability of proteins to undergo conformational switching is central to protein function. For example, conformational changes often accompany enzyme–ligand or protein–protein binding.[27−29] A folding protein will sample many conformations as it progresses toward the folded structure.[30] Proteins can undergo large conformational changes that occur on longer, millisecond to second, time scales. However, these large conformational changes consist of a vast number of more local elementary conformational steps involving small scale structural fluctuations of individual amino acids that can occur on much faster time scales.

The experimental determination of the time scales of elementary conformational steps is a long-standing problem that has now been successfully addressed using ultrafast 2D IR vibrational echo chemical exchange spectroscopy.[14,21,23]

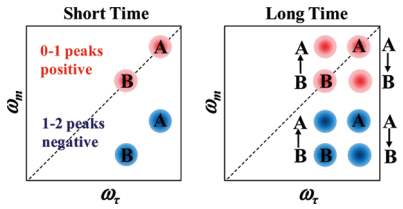

FIGURE 3. Schematic of 2D IR spectra illustrating chemical exchange.

Conformational switching has been studied extensively in the protein myoglobin (Mb) with the ligand CO bound at the active site (MbCO).[14,21,23,31,32] The Fourier transform infrared (FT IR) spectrum of the heme-ligated CO stretching mode of Mb has two major absorption bands, denoted A_1 (1945 cm^{-1}) and A_3 (1932 cm^{-1}), and a third small band, A_0 (1965 cm^{-1}) (Figure 2B).[33] Only the A_1 and A_3 bands will be discussed here. These bands reflect conformational substates of Mb where the distal histidine residue, His64, adopts different configurations (Figure 2A).[33−35]

MbCO rapidly interconverts between the A_1 and A_3 states under thermal equilibrium conditions. CO binding rate constants following photolysis determined at low temperature and extrapolated to ambient temperature indicated the switching between A_1 and A_3 to be <1 ns.[36] Molecular dynamics (MD) simulations have placed the A_1-A_3 switching time on the order of a few hundred picoseconds.[21,23,35]

Here, direct measurements of the A_1-A_3 interconversion time for two Mb mutants under thermal equilibrium conditions using 2D-IR vibrational echo chemical exchange spectroscopy are described. This method has proven useful for studying fast dynamical processes in liquids.[24,26,37,38] The 2D IR vibrational echo chemical exchange experiment is akin to a 2D NMR chemical exchange experiment except that it can operate on a picosecond time scale, and it directly probes the structural degrees of freedom through the time evolution of the 2D vibrational spectrum.

Figure 3 shows a schematic illustration of spectra for an ideal 2D IR chemical exchange experiment. There are two species, A and B, with absorption frequencies, ω_A and ω_B. At short time (left panel), prior to any chemical exchange, two peaks appear on the diagonal that arise from the 0–1 vibrational transitions (red, positive going), and two corresponding peaks appear below, shifted to lower frequency along the ω_m axis by the vibrational anharmonicity, due to vibrational echo emission at the 1–2 transition frequency (blue, negative going). At long time (right panel), chemical exchange has occurred. Some A's have turned into B's, and because the system is in equilibrium, the same number of B's have turned into A's. The chemical exchange is manifested

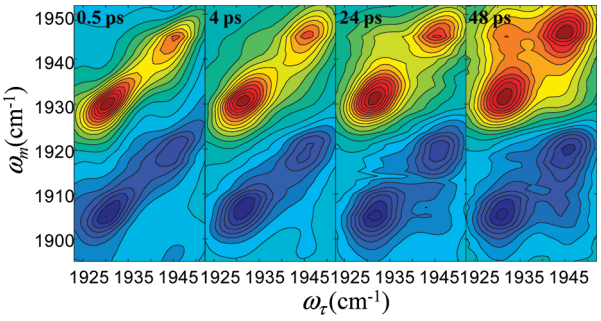

FIGURE 4. Two-dimensional IR spectra of CO in L29I Mb at several waiting times.

by the growth of the off-diagonal peaks. Measurement of the time-dependent increase in the off-diagonal peaks enables determination of the time scale of chemical exchange.[24]

Because the A_3 absorption peak of wild-type MbCO is relatively weak compared with the A_1 peak, which results in the A_1 peak dominating the spectra, we performed the experiments on two Mb mutants, L29I and the double mutant T67R/S92D. These mutations cause the A_1 and A_3 bands in the FT IR spectrum to be approximately the same amplitude (Figure 2B), which helped us to clearly discern all the diagonal and off-diagonal chemical exchange peaks and facilitated their analysis.

Figure 4 displays 2D IR spectra of CO bound to L29I Mb at several T_w's.[14] The data have been normalized to the largest peak at each T_w. Consider the spectrum for $T_w = 0.5$ ps. The two bands on the diagonal (red) correspond to the A_3 and A_1 bands in the absorption spectrum (Figure 2B). The off-diagonal bands (blue) centered at (ω_τ, ω_m) = (1932 cm^{-1}, 1908 cm^{-1}) and (1945 cm^{-1}, 1922 cm^{-1}) result from vibrational echo emission at the 1−2 vibrational transitions of the A_3 and A_1 substates, respectively. The spectrum at T_w = 0.5 ps shows no cross peaks because 0.5 ps is short relative to the conformational switching time.

In contrast, by $T_w = 48$ ps (Figure 4, right panel), sufficient time has elapsed for conformational switching to occur to a significant extent. The conformational switching is manifested by the growth of cross peaks,[24] which are most apparent to the upper left of the 0−1 bands and to the lower right of the 1−2 bands. These cross peaks correspond to the A_3 to A_1 and A_1 to A_3 interconversion, respectively. The overlap of the positive and negative going bands reduces the amplitudes of the other two cross peaks, that is at (ω_τ, ω_m) = (1945 cm^{-1}, 1932 cm^{-1}) and (ω_τ, ω_m) = (1932 cm^{-1}, 1922 cm^{-1}). The 2D IR spectra for T67R/S92D MbCO have a similar appearance.[23]

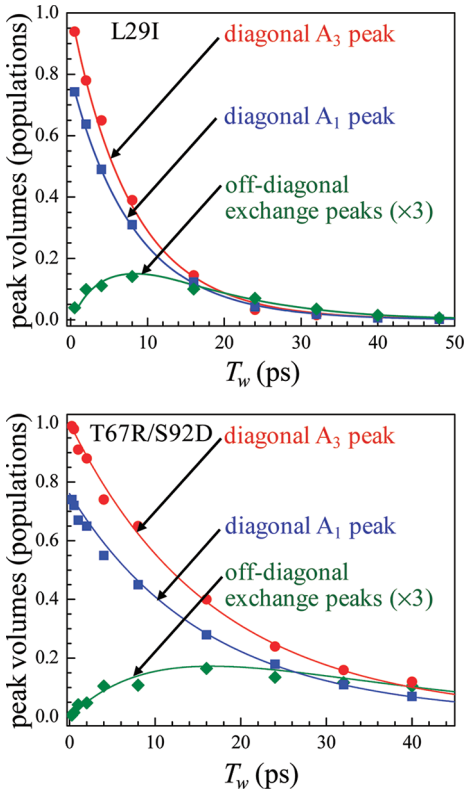

FIGURE 5. Time-dependent changes in the populations of the diagonal and exchange peaks in the 2D IR spectra of CO in L29I (upper) and T67R/S92D (lower) Mb.

The time-dependent 2D IR spectra can be analyzed to quantitatively extract the time constant for the conformational switching. Although the time evolution of the 2D spectra including spectral diffusion and chemical exchange can be calculated using response function theory, it was previously demonstrated that the exchange rate can be extracted using a simpler method.[25] The populations of the conformations are reflected by the integrated volumes of their bands. Because spectral diffusion does not change the peak volumes, only their shapes, at each T_w the volumes can determined by fitting all of the peaks to 2D Gaussian functions.[24,25] Conformational exchange causes the original peaks to decrease in volume and the cross peaks to increase in volume. Concurrently, vibrational and orientational relaxation lead to the decay of all bands with increasing T_w. The time-dependent populations from the peak volumes can be fit with a previously described kinetic model to obtain the time constant of conformational switching.[24,25,38]

Figure 5 displays the chemical exchange data for the two MbCO variants.[14,23] The data (points) show the decay of the diagonal peaks and the growth and decay of the off-diagonal chemical exchange peaks. The solid lines through the data for each mutant are obtained from a fit employing only a

single adjustable parameter, the conformational switching time for the interconversion between the A_1 and A_3 substates. The fits yielded conformational switching times of 47 ± 8 ps and 76 ± 10 ps for L29I and T67R/S92D MbCO, respectively.

The vibrational echo experiments can be combined with MD simulations to better elucidate the structural changes associated with the A_1/A_3 conformational switching.[21,35] As discussed above, rotation of the imidazole side group of His64 is directly involved in creating the difference in the frequencies of the A_1 and A_3 absorption bands. This structural change is supported by high-resolution crystal structures of MbCO that show evidence for two His64 conformations.[34,39] Moreover, an additional Xe binding site distant from the heme iron has been observed in crystal structures of the A_3 conformation of Mb, indicating the presence of a cavity not found in the A_1 state.[40] This suggests that the A_1/A_3 interconversion involves significantly more motion than the rotation of the imidazole side group of His64.

The 2D IR chemical exchange studies of substate switching in the two Mb variants demonstrate that elementary structural changes in proteins can occur on fast time scales. The results presented here show that the time scale can be faster than 100 ps. Motions on similarly fast, subnanosecond time scales also have been characterized through extensive NMR relaxation studies of protein backbone and side chains.[4,41] The NMR experiments can provide order parameters that reflect the angular restriction of backbone and methyl group side chain motion for residues throughout a protein on time scales faster than the protein's global macromolecular tumbling time (typically tens of nanoseconds). These studies suggest that fast internal protein motions contribute significantly to protein function, for instance, from their involvement in the conformational entropy of protein−protein binding[9] and in the allosteric control of molecular recognition.[8]

B. The Influence of Substrate Binding on the Dynamics of $P450_{cam}$ Observed with Spectral Diffusion Measurements. Protein dynamics are thought to play an important role in the activity of P450s,[42−44] a family of monooxygenases of substantial biological and medicinal importance.[45] P450s display a remarkable ability to act on substrates that can differ vastly in their size, structure, and chemical nature.[46] The specificity of their activity for different substrates varies widely for individual enzymes of the family. Structural studies suggest the promiscuity of P450s results from the high plasticity of their active sites.[27−29] Although large structural changes are sometimes observed, often substrate binding leads to only localized changes in protein structure.[47−49] The motions involved in these smaller structural changes occur on fast time scales that have been historically difficult to investigate.

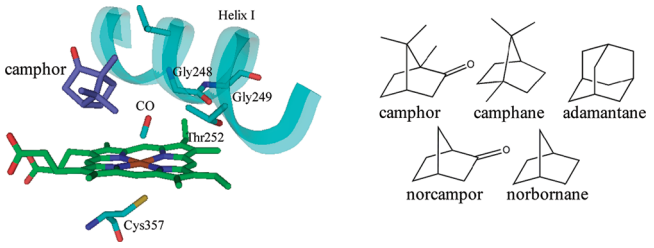

FIGURE 6. Structure of the active site of $P450_{cam}$ (pdb id 1T87) (left) and substrates of complexes studied (right).

Among P450s, the paradigmatic $P450_{cam}$ from *Pseudomonas putida* shows relatively high specificity for small hydrophobic compounds similar to its physiological substrate, camphor.[50] The high specificity is thought to result from relatively constrained active site dynamics.[43,47] While $P450_{cam}$ does act on a number of compounds, lower substrate binding affinity and stereo/regioselectivity of hydroxylation are observed compared with camphor, the natural substrate.[51−53] Calculations suggest that the variations in activity cannot be explained by differences in the chemical reactivity of the substrates, rather that the fluctuating protein environment contributes substantially to the differences.[54] The involvement of protein motions in controlling the selectivity of hydroxylation was examined by characterizing the dynamics of $P450_{cam}$−CO bound to substrates with mild variations from the camphor structure (camphane, adamantane, norcamphor, and norbornane, Figure 6).

Protein structural fluctuations cause the CO stretch frequency to evolve in time, leading to spectral diffusion. The structural changes of the proteins are connected to T_w-dependent changes in the 2D band shapes caused by spectral diffusion via the frequency−frequency correlation function (FFCF). The center line slope (CLS) method provides an accurate way to determine the FFCF from 2D and linear spectra.[55,56] It has been shown theoretically that the T_w-dependent part of the normalized FFCF is directly related to the T_w dependence of the slope of the center line.[55,56] Thus the slope of the center line, the CLS, will vary between a maximum of 1 at $T_w = 0$ and 0 in the limit of sufficiently long waiting time. Detailed procedures for converting the CLS measurement into the FFCF have been described previously.[55,56]

The multiple time scale dynamics are often modeled by a multiexponential form of the FFCF, $C(t)$.

$$C(t) = \sum_{i=1}^{n} \Delta_i^2 \, e^{-t/\tau_i} \qquad (1)$$

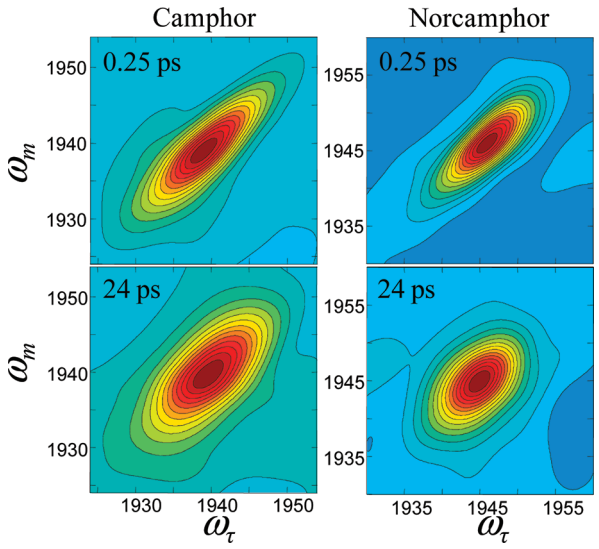

FIGURE 7. Two-dimensional IR spectra of CO in P450$_{cam}$ bound to camphor (left) and norcamphor (right) at two waiting times.

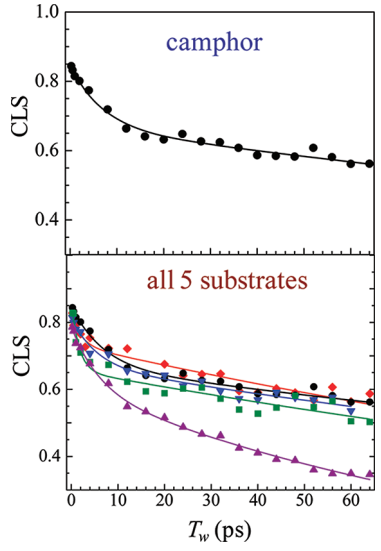

FIGURE 8. CLS decays and corresponding exponential fits for CO in P450$_{cam}$ bound to camphor (upper) and to all substrates studied (lower).

For the *i*th dynamical process, Δ_i is the range of CO frequencies sampled due to protein structural fluctuations and τ_i is the time constant of these fluctuations. This form of the FFCF has been widely used and in particular found applicable in studies of the structural dynamics of heme–CO proteins.[15,16,21,35,57] If $\Delta\tau < 1$ for one component of the FFCF, then Δ and τ cannot be determined separately but rather give rise to a motionally narrowed homogeneous contribution to the absorption spectrum. The presence of a homogeneous contribution causes the initial value of the CLS to be less than 1 at $T_w = 0$. By combining the CLS with the linear absorption spectrum, the full FFCF can be obtained including the homogeneous component.

TABLE 1. Dynamic Parameters from 2D IR Spectra and Dissociation Constants

substrate	T_2 (ps)	Δ_1 (cm^{-1})	τ_1 (ps)	Δ_2 (cm^{-1})	τ_2 (ps)	K_D (μM)
camphor	4.3 ± 0.8	2.8 ± 0.3	6.8 ± 1.4	5.4 ± 0.2	370 ± 65	0.8[a]
camphane	7.2 ± 2.7	1.8 ± 0.3	5.5 ± 1.8	3.8 ± 0.1	300 ± 60	1.1[a]
adamantane	6.3 ± 0.8	2.3 ± 0.3	1.6 ± 0.6	4.1 ± 0.07	260 ± 40	50[b]
norbornane	7.9 ± 0.3	2.4 ± 0.5	2.2 ± 1.2	4.7 ± 0.06	230 ± 30	47[a]
norcamphor	4.9 ± 1.8	1.8 ± 0.1	5.8 ± 1.0	3.2 ± 0.1	110 ± 6	345[a]

[a]Reference 55. [b]Reference 47.

Figure 7 displays 2D IR spectra for data for the camphor and norcamphor P450$_{cam}$–CO complexes at two T_w's. The change in shape of the 2D spectra with time is evident. Figure 8 shows CLS decays for the substrate–P450$_{cam}$ complexes. All of the decays have the same general form. The offsets from 1 at $T_w = 0$ reflect the magnitudes of the homogeneous components. The decays are biexponential, with the fast and slow time constants τ_1 and τ_2, respectively. Table 1 gives the FFCF parameters obtained from the CLS analysis. A complete discussion of the FFCF parameters has been given,[7] although here we will focus only on the slowest decay time, τ_2.

The slowest dynamics measured in this study of P450$_{cam}$ complexes occur on the 100–370 ps time scale (Table 1). The approximately 2-fold larger value of Δ_2 (root mean frequency fluctuation amplitude) compared with Δ_1 for all of the complexes shows that these slower motions make the greatest contribution to the vibrational line width. The slow time scale suggests that this component arises from larger-scale motions than those that give rise to the faster dynamics, likely similar in scale to the 50–100 ps A_1–A_3 switching measured for MbCO.[14,21,23] However, molecular dynamics simulations of MbCO find that dynamics throughout the protein contribute to the FFCF,[57] and this is likely also the case for the FFCFs of the P450$_{cam}$ complexes.

The motions on the hundreds of picosecond time scale are found to be the slowest in P450$_{cam}$ bound to its natural substrate, camphor, implying that the barriers to structural fluctuations on this time scale are greatest for this complex. In comparison, the τ_2 correlation time is several times shorter for the norcamphor complex. From a simple Eyring model of kinetics,[58] comparison of the longer time scale components suggest the barriers to the corresponding structural changes in the camphor complex are roughly 30% greater than those in the norcamphor complex and are consistent with optimal packing of the natural camphor substrate in the P450$_{cam}$ active site. The faster dynamics of the norcamphor

complex indicate relatively low kinetic barriers among structural conformations and hence a smoother energy landscape. Conversely, the slower dynamics in the complex with the natural substrate indicate relatively high barriers to motion, leading to the picture of a more "rugged" energy landscape.

The uniquely fast dynamics observed in the norcamphor complex (Table 1) are particularly notable given the low selectivity of the hydroxylation of the norcamphor substrate. While 100% and 90% 5′-exo hydroxylation product are obtained from camphor and camphane, respectively,[52] the activity of $P450_{cam}$ toward norcamphor results in only 60% of the 5′-exo hydroxylation product.[53] (Adamantane and norbornane do not possess an equivalent number of distinct carbon atoms.) The correlation between the dynamics of the complexes and their regioselectivities of hydroxylation is consistent with the involvement of protein dynamics in the selectivity of $P450_{cam}$ activity. While the actual chemical reaction likely involves a low probability incursion to a high energy state, it seems plausible that the more rugged landscape would serve to restrict the particular sequences of structural fluctuations that can lead to the transition state, and thus enhance the selectivity of camphor hydroxylation. In contrast, the smoother energy landscape of the norcamphor complex may lead to a more permissive trajectory to the transition state and thus allow the reaction to proceed with "incorrect" carbon centers.

In addition, the 2D IR results suggest that the dynamics of the complexes may influence the binding affinity, because the dissociation constants and τ_2 are also generally correlated. Those substrates with smaller K_D values for binding to $P450_{cam}$ show longer τ_2 times in the FFCFs of the substrate complexes (Table 1). Thus the binding affinity increases with slower dynamics. This effect is not likely due to conformational entropy changes upon binding, because more constrained substrate complexes should lead to greater entropic penalties for binding. It is more likely that the higher barriers that result in slower dynamics are due to more enthalpically favorable interactions within the tighter complexes.

Two-dimensional IR vibrational echo spectroscopy measured dynamics in $P450_{cam}$ complexes on a wide range of time scales. The complex with the natural substrate, camphor, shows slower motions compared with the unnatural substrate complexes, indicating higher barriers to protein structural changes. The enzyme likely has evolved to optimally bind camphor to restrict the structural fluctuations that may lead to the transition state, such that hydroxylation occurs only at a specific carbon center. Thus, overall the data support the involvement of fast structural dynamics in enzyme function, and in particular, the specificity of hydroxylation by $P450_{cam}$.

Similarly fast motions have been observed in other enzymes with spectral diffusion measurements employing small ligand IR probes.[18,59,60] Motions on the tens of picoseconds time scale were observed in 2D vibrational studies of azide bound to carbonic anhydrase[60] and a small molecule nitrile inhibitor bound to HIV reverse transcriptase.[59] In a study of azide, a transition state analog, bound to formate dehydrogenase in several substrate/cofactor complexes, slower motions observed in the binary ligand complex of formate dehydrogenase disappeared upon forming the reactant and product ternary complexes,[18] suggesting that protein motions on fast, subnanosecond time scales might impact enzyme molecular recognition, in accord with the $P450_{cam}$ study described here.

IV. Concluding Remarks

The application of two techniques of ultrafast 2D IR vibrational echo spectroscopy to the study of proteins has been described. One method, chemical exchange spectroscopy, was used to directly observe the interconversion between distinct structural substates of two Mb mutants. In both cases, conformational switching times less than 100 ps were measured, demonstrating that basic structural changes in proteins can occur on fast time scales.

In the second application, 2D IR vibrational echo experiments were used to measure spectral diffusion, which is directly related to protein structural fluctuations. The dynamics of $P450_{cam}$ in complex with CO and five different substrates were discussed. The slowest components of the fast structural fluctuations show correlations with the selectivity of the activity and the binding constants of the substrates with the enzyme. These results indicate that an enzyme's fast structural fluctuations are intimately involved in biological processes that occur on time scales that are many orders of magnitude slower.

The applications of 2D IR spectroscopy to the measurement of protein dynamics presented here used a heme-bound CO ligand as a vibrational probe. To generalize the methods of 2D IR spectroscopy to study dynamics of proteins beyond those that bind small molecule ligands and to measure the dynamics at sites throughout protein structures, our group has begun to combine the spectroscopic methods with the site-specific incorporation of amino acids that bear vibrational probe groups.[13,15] Azido, cyano, and carbon-deuterium labeled amino acids can be

introduced at specific sites in proteins to exploit their infrared frequencies around 2000 cm^{-1} in a relatively transparent region of a protein IR spectrum,[13,15,61] permitting the discernment and analysis of absorption bands due single residues in proteins. Cyanophenylalanine has been employed in 2D IR studies of peptide dynamics and folding.[15] Recently, our group reported the first study of the dynamics of a labeled amino acid, azidophenylalanine, in a full length protein, myoglobin.[13] The combination of site-specific protein labeling and 2D IR spectroscopy promises to be a powerful means of understanding the role of dynamics in protein function.

We thank the National Institutes of Health (Grant 2-R01-GM061137-09) for support of this research. M.C.T. also thanks the National Institutes of Health for a postdoctoral fellowship (Grant F32-GM090549).

BIOGRAPHICAL INFORMATION

Megan C. Thielges received her B.S. (2003) from Arizona State University and Ph.D. (2009) from the Scripps Research Institute. She is currently a NIH postdoctoral fellow in the Fayer group at Stanford University and will join the chemistry faculty at Indiana University in the fall of 2012.

Michael D. Fayer received his B.S. (1969) and Ph.D. (1974) from the University of California at Berkeley. He joined the faculty at Stanford University in 1974, where he is the David Mulvane Ehrsam and Edward Curtis Franklin Professor of Chemistry. He is a member of the National Academy of Science, and he has received the E. Bright Wilson Award for Spectroscopy, the Ellis R. Lippincott Award, the Earl K. Plyler Prize for Molecular Spectroscopy, and the Arthur L. Schawlow Prize in Laser Science.

FOOTNOTES

The authors declare no competing financial interest.

†Department of Chemistry, Indiana University, Bloomington, Indiana 47405, United States.

REFERENCES

1 Henzler-Wildman, K. A.; Lei, M.; Thai, V.; Kerns, S. J.; Karplus, M.; Kern, D. A. Hierarchy of Timescales in Protein Dynamics Is Linked to Enzyme Catalysis. *Nature* **2007**, *450*, 913–916.

2 Hammes-Schiffer, S.; Benkovic, S. J. Relating Protein Motion to Catalysis. *Annu. Rev. Biochem.* **2006**, *75*, 519–541.

3 Erzberger, J. P.; Berger, J. M. Evolutionary Relationships and Structural Mechanisms of AAA+ Proteins. *Annu. Rev. Biophys. Biomol. Struct.* **2006**, *35*, 93–114.

4 Boehr, D. D.; Dyson, H. J.; Wright, P. E. An NMR Perspective on Enzyme Dynamics. *Chem. Rev.* **2006**, *106*, 3055–3079.

5 Frauenfelder, H.; Sligar, S. G.; Wolynes, P. G. The Energy Landscapes and Motions of Proteins. *Science* **1991**, *254*, 1598–1603.

6 Parak, F.; Frauenfelder, H. Protein Dynamics. *Physica A* **1993**, *201*, 332–345.

7 Thielges, M. C.; Chung, J. K.; Fayer, M. D. Protein Dynamics in Cytochrome P450 Molecular Recognition and Substrate Specificity Using 2D IR Vibrational Echo Spectroscopy. *J. Am. Chem. Soc.* **2011**, *133*, 3995–4004.

8 Petit, C. M.; Zhang, J.; Sapienza, P. J.; Fuentes, E. J.; Lee, A. L. Hidden Dynamic Allostery in a PDZ Domain. *Proc. Natl. Acad. Sci. U.S.A.* **2009**, *106*, 18249–18254.

9 Frederick, K. K.; Marlow, M. S.; Valentine, K. G.; Wand, A. J. Conformational Entropy in Molecular Recognition by Proteins. *Nature* **2007**, *448*, 325–329.

10 Jimenez, R.; Salazar, G.; Yin, J.; Joo, T.; Romesberg, F. E. Protein Dynamics and the Immunological Evolution of Molecular Recognition. *Proc. Natl. Acad. Sci. U.S.A.* **2004**, *101*, 3803–3808.

11 Hong, M. K.; Braunstein, D.; Cowen, B. R.; Frauenfelder, H.; Iben, I. E. T.; Mourant, J. R.; Ormos, P.; Scholl, R.; Schulte, A.; Steinbach, P. J.; Xie, A. H.; Young, R. D. Conformational Substates and Motions in Myoglobin - External Influences on Structure and Dynamics. *Biophys. J.* **1990**, *58*, 429–436.

12 Frauenfelder, H.; McMahon, B. H.; Austin, R. H.; Chu, K.; Groves, J. T. The Role of Structure, Energy Landscape, Dynamics, and Allostery in the Enzymatic Function of Myoglobin. *Proc. Natl. Acad. Sci. U.S.A.* **2001**, *98*, 2370–2374.

13 Thielges, M. C.; Axup, J. Y.; Wong, D.; Lee, H. S.; Chung, J. K.; Schultz, P. G.; Fayer, M. D. Two-Dimensional IR Spectroscopy of Protein Dynamics Using Two Vibrational Labels: A Site-Specific Genetically Encoded Unnatural Amino Acid and an Active Site Ligand. *J. Phys. Chem. B* **2011**, *115*, 11294–11304.

14 Ishikawa, H.; Kwak, K.; Chung, J. K.; Kim, S.; Fayer, M. D. Direct Observation of Fast Protein Conformational Switching. *Proc. Natl. Acad. Sci. U.S.A.* **2008**, *105*, 8619–8624.

15 Chung, J. K.; Thielges, M. C.; Fayer, M. D. Dynamics of the Folded and Unfolded Villin Headpiece (HP35) Measured with Ultrafast 2D IR Vibrational Echo Spectroscopy. *Proc. Natl. Acad. Sci. U.S.A.* **2011**, *108*, 3578–3583.

16 Chung, J. K.; Thielges, M. C.; Bowman, S. E. J.; Bren, K. L.; Fayer, M. D. Temperature Dependent Equilibrium Native to Unfolded Protein Dynamics and Properties Observed with IR Absorption and 2D IR Vibrational Echo Experiments. *J. Am. Chem. Soc.* **2011**, *133*, 6681–6691.

17 Ganim, Z.; Chung, H. S.; Smith, A. W.; Deflores, L. P.; Jones, K. C.; Tokmakoff, A. Amide I Two-Dimensional Infrared Spectroscopy of Proteins. *Acc. Chem. Res.* **2008**, *41*, 432–441.

18 Bandaria, J. N.; Dutta, S.; Nydegger, M. W.; Rock, W.; Kohen, A.; Cheatum, C. M. Characterizing the Dynamics of Functionally Relevant Complexes of Formate Dehydrogenase. *Proc. Natl. Acad. Sci. U.S.A.* **2010**, *107*, 17974–17979.

19 Middleton, C. T.; Woys, A. M.; Mukherjee, S. S.; Zanni, M. T. Residue-Specific Structural Kinetics of Proteins through the Union of Isotope Labeling, Mid-IR Pulse Shaping, and Coherent 2D IR Spectroscopy. *Methods* **2010**, *52*, 12–22.

20 Kim, Y. S.; Hochstrasser, R. M. Applications of 2D IR Spectroscopy to Peptides, Proteins, and Hydrogen-Bond Dynamics. *J. Phys. Chem. B* **2009**, *113*, 8231–8251.

21 Bagchi, S.; Nebgen, B. T.; Loring, R. F.; Fayer, M. D. Dynamics of a Myoglobin Mutant Enzyme: 2D IR Vibrational Echo Experiments and Simulations. *J. Am. Chem. Soc.* **2010**, *132*, 18367–18376.

22 Park, S.; Kwak, K.; Fayer, M. D. Ultrafast 2D-IR Vibrational Echo Spectroscopy: A Probe of Molecular Dynamics. *Laser Phys. Lett.* **2007**, *4*, 704–718.

23 Bagchi, S.; Thorpe, D. G.; Thorpe, I. F.; Voth, G. A.; Fayer, M. D. Conformational Switching between Protein Substates Studied with 2D IR Vibrational Echo Spectroscopy and Molecular Dynamics Simulations. *J. Phys. Chem. B* **2010**, *114*, 17187–17193.

24 Zheng, J.; Kwak, K.; Asbury, J. B.; Chen, X.; Piletic, I.; Fayer, M. D. Ultrafast Dynamics of Solute-Solvent Complexation Observed at Thermal Equilibrium in Real Time. *Science* **2005**, *309*, 1338–1343.

25 Kwak, K.; Zheng, J.; Cang, H.; Fayer, M. D. Ultrafast 2D IR Vibrational Echo Chemical Exchange Experiments and Theory. *J. Phys. Chem. B.* **2006**, *110*, 19998–20013.

26 Moilanen, D. E.; Wong, D.; Rosenfeld, D. E.; Fenn, E. E.; Fayer, M. D. Ion-Water Hydrogen Bond Switching Observed with 2D IR Vibrational Echo Chemical Exchange Spectroscopy. *Proc. Nat. Acad. Sci. U.S.A.* **2009**, *106*, 375–380.

27 Scott, E. E.; He, Y. A.; Wester, M. R.; White, M. A.; Chin, C. C.; Halpert, J. R.; Johnson, E. F.; Stout, C. D. An Open Conformation of Mammalian Cytochrome P450 2B4 at 1.6- Angstrom Resolution. *Proc. Natl. Acad. Sci. U.S.A.* **2003**, *100*, 13196–13201.

28 Poulos, T. L.; Johnson, E. F. In *Cytochrome P450: Structure, Mechanism, and Biochemistry*; de Montellano, O., Ed.; Plenum Press: New York, 2005; Vol. 3; pp 87−114.

29 Ekroos, M.; Sjögren, T. Structural Basis for Ligand Promiscuity in Cytochrome P450 3A4. *Proc. Natl. Acad. Sci. U.S.A.* **2006**, *103*, 13682–13687.

30 Oliveberg, M.; Wolynes, P. G. The Experimental Survey of Protein-Folding Energy Landscapes. *Q. Rev. Biophys.* **2005**, *38*, 245–288.

31 Ansari, A.; Beredzen, J.; Braunstein, D.; Cowen, B. R.; Frauenfelder, H.; Hong, M. K.; Iben, I. E. T.; Johnson, J. B.; Ormos, P.; Sauke, T.; Schroll, R.; Schulte, A.; Steinback, P. J.; Vittitow, J.; Young, R. D. Rebinding and Relaxation in the Myoglobin Pocket. *Biophys. Chem.* **1987**, *26*, 337–355.

32 Muller, J. D.; McMahon, B. H.; Chen, E. Y. T.; Sligar, S. G.; Nienhaus, G. U. Connection between the Taxonomic Substates of Protonation of Histidines 64 and 97 in Carbonmonoxy Myoglobin. *Biophys. J.* **1999**, *77*, 1036–1051.

33 Li, T. S.; Quillin, M. L.; Phillips, G. N., Jr.; Olson, J. S. Structural Determinants of the Stretching Frequency of CO Bound to Myoglobin. *Biochemistry* **1994**, *33*, 1433–1446.

34 Vojtechovsky, J.; Chu, K.; Berendzen, J.; Sweet, R. M.; Schlichting, I. Crystal Structures of Myoglobin-Ligand Complexes at near Atomic Resolution. *Biophys. J.* **1999**, *77*, 2153–2174.

35 Merchant, K. A.; Noid, W. G.; Akiyama, R.; Finkelstein, I. J.; Goun, A.; McClain, B. L.; Loring, R. F.; Fayer, M. D. Myoglobin-CO Substate Structures and Dynamics: Multidimensional

Vibrational Echoes and Molecular Dynamics Simulations. *J. Am. Chem. Soc.* **2003**, *125*, 13804–13818.

36 Johnson, J. B.; Lamb, D. C.; Frauenfelder, H.; Müller, J. D.; McMahon, B.; Nienhaus, G. U.; Young, R. D. Ligand Binding to Heme Proteins. 6. Interconversion of Taxonomic Substates in Carbonmonoxymyoglobin. *Biophys. J.* **1996**, *71*, 1563–1573.

37 Kim, Y. S.; Hochstrasser, R. M. Chemical Exchange 2D IR of Hydrogen-Bond Making and Breaking. *Proc. Natl. Acad. Sci. U.S.A.* **2005**, *102*, 11185–11190.

38 Zheng, J.; Kwak, K.; Xie, J.; Fayer, M. D. Ultrafast Carbon-Carbon Single Bond Rotational Isomerization in Room Temperature Solution. *Science* **2006**, 1951–1955.

39 Teeter, M. M. Myoglobin Cavities Provide Interior Ligand Pathway. *Protein Sci.* **2004**, *13*, 313–318.

40 Tilton, R. F., Jr.; Kuntz, I. D., Jr.; Petsko, G. A. Cavities in Proteins: Structure of a Metmyoglobin−Xenon Complex Solved to 1.9 Å. *Biochemistry* **1984**, *23*, 2849–2857.

41 Igumenova, T. I.; Frederick, K. K.; Wand, A. J. Characterization of the Fast Dynamics of Protein Amino Acid Side Chains Using NMR Relaxation in Solution. *Chem. Rev.* **2006**, *106*, 1672–1699.

42 Skopalík, J.; Anzenbacher, P.; Otyepka, M. Flexibility of Human Cytochromes P450: Molecular Dynamics Reveals Differences between Cyps 3A4, 2C9, and 2A6, Which Correlate with Their Substrate Preferences. *J. Phys. Chem. B* **2008**, *112*, 8165–8173.

43 Winn, P. J.; Lüdemann, S. K.; Gauges, R.; Lounnas, V.; Wade, R. C. Comparison of the Dynamics of Substrate Access Channels in Three Cytochrome P450s Reveals Different Opening Mechanisms and a Novel Functional Role for a Buried Arginine. *Proc. Natl. Acad. Sci. U.S.A.* **2002**, *99*, 5361–5366.

44 Wade, R. C.; Motiejunas, D.; Schleinkofer, K.; Sudarko; Winn, P. J.; Banerjee, A.; Kariakin, A.; Jung, C. Multiple Molecular Recognition Mechanisms. Cytochrome P450-- a Case Study. *Biochim. Biophys. Acta* **2005**, *1754*, 239–244.

45 Guengerich, F. P. Cytochrome P450 and Chemical Toxicology. *Chem. Res. Toxicol.* **2008**, *21*, 70–83.

46 Schuler, M. A.; Sligar, S. G. In *The Ubiquitous Roles of the Cytochromes: Metal Ions in Life Sciences*; Sigel, A., Sigel, H., Sigel, R. K. O., Eds.; John Wiley & Sons, Ltd.: West Sussex, 2007; Vol. 3; pp 1−26.

47 Schlichting, I.; Berendzen, J.; Chu, K.; Stock, A. M.; Maves, S. A.; Benson, D. E.; Sweet, B. M.; Ringe, D.; Petsko, G. A.; Sligar, S. G. The Catalytic Pathway of Cytochrome P450cam at Atomic Resolution. *Science* **2000**, *287*, 1615–1622.

48 Williams, P. A.; Cosme, J.; Vinkovic, D. M.; Ward, A.; Angove, H. C.; Day, P. J.; Vonrhein, C.; Tickle, I. J.; Jhoti, H. Crystal Structures of Human Cytochrome P450 3A4 Bound to Metyrapone and Progesterone. *Science* **2004**, *305*, 683–686.

49 Sakurai, K.; Shimada, H.; Hayashi, T.; Tsukihara, T. Substrate Binding Induces Structural Changes in Cytochrome P450cam. *Acta Crystallogr.* **2009**, *F65*, 80–83.

50 Harris, D.; Loew, G. Prediction of Regiospecific Hydroxylation of Camphor Analogs by Cytochrome-$P450_{cam}$ *J. Am. Chem. Soc.* **1995**, *117*, 2738–2746.

51 White, R. E.; Mccarthy, M. B.; Egeberg, K. D.; Sligar, S. G. Regioselectivity in the Cytochromes-P-450 - Control by Protein Constraints and by Chemical Reactivities. *Arch. Biochem. Biophys.* **1984**, *228*, 493–502.

52 Atkins, W. M.; Sligar, S. G. The Roles of Active-Site Hydrogen-Bonding in Cytochrome P-450cam as Revealed by Site-Directed Mutagenesis. *J. Biol. Chem.* **1988**, *263*, 18842–18849.

53 Loida, P. J.; Sligar, S. G.; Paulsen, M. D.; Arnold, G. E.; Ornstein, R. L. Stereoselective Hydroxylation of Norcamphor by Cytochrome-$P450_{cam}$ - Experimental-Verification of Molecular-Dynamics Simulations. *J. Biol. Chem.* **1995**, *270*, 5326–5330.

54 Collins, J. R.; Loew, G. H. Theoretical-Study of the Product Specificity in the Hydroxylation of Camphor, Norcamphor, 5,5-Difluorocamphor, and Pericyclocamphanone by Cytochrome-P-450cam. *J. Biol. Chem.* **1988**, *263*, 3164–3170.

55 Kwak, K.; Park, S.; Finkelstein, I. J.; Fayer, M. D. Frequency-Frequency Correlation Functions and Apodization in Two-Dimensional Infrared Vibrational Echo Spectroscopy: A New Approach. *J. Chem. Phys.* **2007**, *127*, No. 124503.

56 Kwak, K.; Rosenfeld, D. E.; Fayer, M. D. Taking Apart the Two-Dimensional Infrared Vibrational Echo Spectra: More Information and Elimination of Distortions. *J. Chem. Phys.* **2008**, *128*, No. 204505.

57 Massari, A. M.; Finkelstein, I. J.; McClain, B. L.; Goj, A.; Wen, X.; Bren, K. L.; Loring, R. F.; Fayer, M. D. The Influence of Aqueous Versus Glassy Solvents on Protein Dynamics: Vibrational Echo Experiments and Molecular Dynamics Simulations. *J. Am. Chem. Soc.* **2005**, *127*, 14279–14289.

58 Eyring, H. The Activated Complex in Chemical Reactions. *J. Chem. Phys.* **1935**, *3*, 107–115.

59 Fang, C.; Bauman, J. D.; Das, K.; Remorino, A.; Arnold, E.; Hochstrasser, R. M. Two-Dimensional Infrared Spectra Reveal Relaxation of the Nonnucleoside Inhibitor TMC278 Complexed with HIV-1 Reverse Transcriptase. *Proc. Natl. Acad. Sci. U.S.A.* **2008**, *105*, 1472–1477.

60 Lim, M.; Hamm, P.; Hochstrasser, R. M. Protein Fluctuations Are Sensed by Stimulated Infrared Echoes of the Vibrations of Carbon Monoxide and Azide Probes. *Proc. Natl. Acad. Sci. U.S.A.* **1998**, *95*, 15315–15320.

61 Chin, J. K.; Jimenez, R.; Romesberg, F. E. Direct Observation of Protein Vibrations by Selective Incorporation of Spectroscopically Observable Carbon−Deuterium Bonds in Cytochrome *C. J. Am. Chem. Soc.* **2001**, *123*, 2426–2427.